Interventional MRI-guided Putaminal Delivery of AAV2-GDNF for a Planned Clinical Trial in Parkinson's Disease

R Mark Richardson[1], Adrian P Kells[1], Kathryn H Rosenbluth[1], Ernesto Aguilar Salegio[1], Massimo S Fiandaca[1], Paul S Larson[1], Philip A Starr[1], Alastair J Martin[2], Russell R Lonser[3], Howard J Federoff[4,5], John R Forsayeth[1] and Krystof S Bankiewicz[1]

[1]Department of Neurological Surgery, University of California San Francisco, San Francisco, California, USA; [2]Department of Radiology, University of California San Francisco, San Francisco, California, USA; [3]Surgical Neurology Branch, National Institute of Neurological Disorders and Stroke, Bethesda, Maryland, USA; [4]Department of Neurology, Georgetown University Medical Center, Washington, District of Columbia, USA; [5]Department of Neuroscience, Georgetown University Medical Center, Washington, District of Columbia, USA

Clinical trials involving direct infusion of neurotrophic therapies for Parkinson's disease (PD) have suffered from poor coverage of the putamen. The planned use of a novel interventional-magnetic resonance imaging (iMRI) targeting system for achieving precise, real-time convection-enhanced delivery in a planned clinical trial of adeno-associated virus serotype 2 (AAV2)-glial-derived neurotrophic factor (GDNF) in PD patients was modeled in nonhuman primates (NHP). NHP received bilateral coinfusions of gadoteridol (Gd)/AAV2-GDNF into two sites in each putamen, and three NHP received larger infusion volumes in the thalamus. The average targeting error for cannula tip placement in the putamen was <1 mm, and adjacent putamenal infusions were distributed in a uniform manner. GDNF expression patterns in the putamen were highly correlated with areas of Gd distribution seen on MRI. The distribution volume to infusion volume ratio in the putamen was similar to that in the thalamus, where larger infusions were achieved. Modeling the placement of adjacent 150 and 300 µl thalamic infusions into the three-dimensional space of the human putamen demonstrated coverage of the postcommissural putamen, containment within the striatum and expected anterograde transport to globus pallidus and substantia nigra pars reticulata. The results elucidate the necessary parameters for achieving widespread GDNF expression in the putamenal motor area and afferent substantia nigra of PD patients.

Received 4 November 2010; accepted 17 January 2011; published online 22 February 2011. doi:10.1038/mt.2011.11

INTRODUCTION

Despite the efficacy of deep brain stimulation for treating multiple symptoms of Parkinson's disease (PD), this therapy does not slow disease progression. In contrast, gene therapy offers an approach that may alter the disease process directly by inducing the expression of a specific protein that slows or otherwise counteracts dopaminergic neuronal loss. Glial-derived neurotrophic factor (GDNF), a potent biologic that has neurotrophic and neuroprotective effects when delivered to the degenerated striatum,[1,2] has been effective in ameliorating symptoms in Parkinsonian nonhuman primates (NHP) using a gene therapy approach.[3,4] Achieving clinically significant effects in PD patients will require a treatment platform validated to ensure viral vector delivery to the chosen target area and accurate prediction of areas of subsequent GDNF expression.

Previous clinical trials of direct neurotrophic delivery in PD have included intracerebroventricular[5] and intraputamenal[6–8] infusion of GDNF protein, while current efforts include intrastriatal and intranigral transfer of the gene encoding neurturin,[9] a GDNF-related biologic. The adverse events and lack of therapeutic efficacy associated with clinical intracerebroventricular GDNF protein delivery are an illustration of the effects of poor target delivery and resultant dissemination within the cerebrospinal fluid system. In the phase 2 trial of direct intraputamenal GDNF infusion, poor delivery was more than likely was responsible for elevated cerebrospinal fluid levels of GDNF and low putamenal concentrations, resulting in a lack of therapeutic benefit in the phase 2 trial, despite initial positive results in phase 1 trials.[10,11] The formation of antibodies to GDNF in over half of these patients[12] reinforces the concept that protein leakage into the cerebrospinal fluid space and resultant venous system must be avoided in an effort to prevent systemic inoculation and antibody formation, as intrastriatal adeno-associated virus serotype 2 (AAV2)-GDNF delivery does not result in detectable GDNF protein or GDNF antibodies in the cerebrospinal fluid of NHPs.[13] Inadequate delivery and gene expression are also suspected to be responsible for a lack of clinical benefit in patients recently treated in a phase 2 clinical trial of AAV2-neurturin.

Previous work has shown that AAV2-GDNF delivered via convection-enhanced delivery (CED) to the putamen in

Correspondence: *R Mark Richardson, Department of Neurological Surgery, University of California San Francisco, 505 Parnassus Avenue, Room M779, San Francisco, California 94143-0112, USA. E-mail: richardsonma@neuosurg.usf.edu*

overlesioned, clinically stable hemi-Parkinsonian NHP model results in significant and persistent clinical recovery.[3,4] To ensure adequate and reproducible clinical delivery of this gene therapeutic by direct intracerebral infusion, a reliable delivery system must be employed that provides verification of vector delivery to the targeted region. Inconsistent targeting or distribution will compromise safety and limit efficacy, thus rendering clinical data variable and resulting in inconclusive trial outcomes. We have recently described an interventional-magnetic resonance imaging (iMRI)-based platform that employs a skull-mounted aiming device, integrated software system, and customized step-design cannula for real-time targeting and visualization of CED in the brain.[14] Additionally, we have recently shown that gadoteridol (Gd), an MRI contrast agent, is an accurate tracer for visualizing the distribution of and AAV2 vectors and subsequent transgene expression.[15] In this article, we report the use of a novel, US Food and Drug Administration-approved, iMRI-based clinical delivery platform to specifically model, in NHP, a planned GDNF gene therapy trial in PD. We discuss the parameters necessary for safely achieving homogenous GDNF expression within regions of the human Parkinsonian brain necessary for recovery of motor function.

RESULTS

Three NHPs underwent sequential, bilateral delivery of 50–60 µl Gd/AAV2-GDNF to two intraputamenal locations on each side, and three NHP underwent sequential, bilateral delivery of 150, 200, or 300 µl Gd/AAV2-GDNF into the thalami. Accurate cannula placement was achieved on the first attempt (without the need for repositioning) in all cases. No technical limitations were encountered in redirecting the clinical cannula for infusing two putamenal sites within the same hemisphere. No adverse events resulted from the surgical procedure or from the subsequent gene expression. Upon postmortem examination, hematoxylin and eosin stained brain sections revealed no evidence of hemorrhage or significant neuropathology at the infusion sites, other than expected minor glial scarring along the cannula tract.

Performance of delivery platform for putamenal infusions

The guidance system automatically calculated each targeting error, defined as the three-dimensional distance between the expected cannula tip location and the actual location marked by the operator on postinsertion imaging. The skull-mounting aiming device and integrated infusion cannula performed very well. The average targeting error for all 17 infusions was 0.8 mm (95% confidence interval (CI) = 0.2), and there was no difference between the average targeting error for infusions in the putamen (0.8 mm, 95% CI = 0.1, n = 11) versus thalamus (0.7 mm, 95% CI = 0.1, n = 6) (**Table 1**). These calculated errors are approximately equal to the imaging resolution (Voxel size = 0.7 × 0.7 × 1.0 mm). We found that the infusion rate could be increased to rates higher than previously achieved without detrimental effects on volume distribution, *e.g.*, cannula reflux or early leakage into white matter tracts. For putamenal infusions, the infusion rate was increased by 0.5 µl/min every 5 minutes starting at 1 µl/min to reach a maximal rate of 3 µl/min.

Table 1 Targeting accuracy

NHP number	Anatomic target	Target error (mm)	Volume infused (ml)	Vd/Vi
1	p.c. put	0.6	60	4.6
1	c. put	0.9	50	3.3
1	p.c. put	0.5	50	3.3
2	c. put	0.9	50	4.1
2	p.c. put	0.7	50	3.9
2	c. put	1.2	50	2.6[a]
2	p.c. put	0.7	50	2.9[a]
3	c. put	0.5	50	3.9
3	p.c. put	0.6	50	3.5
3	c. put	1.2	50	2.0[a]
3	p.c. put	1.0	50	2.4[a]
4	Thalamus	0.9	160	3.6
4	Thalamus	0.8	200	3.3
5	Thalamus	0.8	200	3.1
5	Thalamus	0.4	200	3.5
6	Thalamus	0.6	300	3.0
6	Thalamus	0.7	300	2.6
Average (±95% CI)		0.8 (±0.2)		3.3 (±0.3)

Abbreviations: CI, confidence interval; c. put, commissural putamen; p.c., postcommissural putamen; MRI, magnetic resonance imaging; NHP, nonhuman primates.
[a]Significant leakage noted on MRI.

The ratio of distribution volume to infusion volume (Vd/Vi) was similar to that reported for the initial validation of this system.[14] The average Vd/Vi was 3.3 (95% CI = 0.5) for all infusions within the putamen and 3.8 (95% CI = 0.5) when infusions in which distribution along an extraputamenal pathway visualized on MRI were excluded (**Table 1**). Distribution out of the putamen was visible in 4 of 11 infusions, due to leakage laterally into the external capsule, dorsally into the internal capsule, or ventrally via perivascular transport along a presumed lenticulostriate artery.[16] In these cases of distribution into white matter tracts, the cannula tip, or cannula step, was likely placed <3 mm from the border of the putamen,[17] as a result of suboptimal MRI resolution.

We demonstrated also that this system could place two infusions in close proximity within the putamen without producing reflux into the initial cannula tract during the course of the second infusion. The average distance between adjacent cannula tip locations was 5 mm. In four of six infused putamen, adjacent infusions produced overlapping areas of Gd distribution, and no gross change in distribution characteristics of the second infusion were noted (**Figure 1**).

Correlation between Gd signal and GDNF expression

GDNF expression closely overlapped areas of Gd signal observed during iMRI in all infusions. Cross-sectional areas of Gd distribution were quantitatively compared to cross-sectional areas of GDNF expression in instances where a corresponding tissue section could be identified that closely matched the anatomy of the MRI slice in the cannula trajectory plane (6 of 11 infusions)

(Figure 2a–c). The average ratio of the cross-sectional area of MRI distribution to the area of GDNF staining was 0.99 (95% CI = 0.04) (Figure 2d). Areas of extrastriatal GDNF expression predicted by the convection of Gd into white mater tracts also were observed. In particular, GDNF expression overlapped the distribution of Gd observed to escape in some infusions into the internal and external capsules, as well as along a presumed lenticulostriate artery pathway (Figure 2b). No significant amount of cell body labeling was observed in white matter tracts, suggesting that GDNF antibody staining in these areas reflected high levels of transgene secretion from transfected neurons in neighboring regions. Note that expression along the needle tract reflected reflux of vector following cannula withdrawal and not cannula reflux, as Gd was only seen in the tract on scans obtained following cannula removal and not during infusions. Including a time delay between completion of the infusion and cannula removal could minimize this late cannula tract reflux.

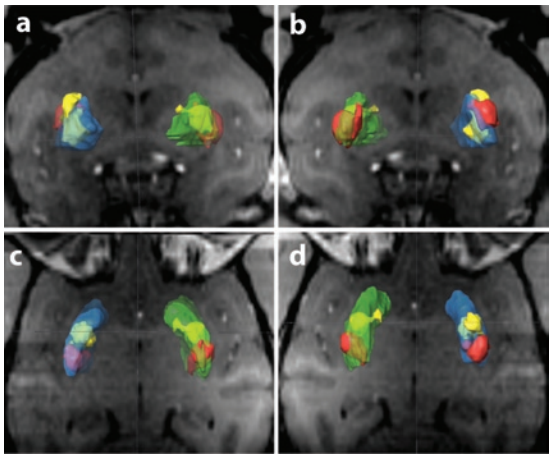

Figure 1 Three-dimensional reconstructions of putamenal infusions. Reconstructions of anterior (yellow) and posterior (red) infusions into both the right (blue) and left (green) putamen in one animal are shown in relation to the MRI plane through the anterior commissure, in the (**a**) anterior to posterior, (**b**) posterior to anterior, (**c**) ventral to dorsal, and (**d**) dorsal to ventral views.

Anterograde transport of the vector and/or transgene product was evident in all infusions. GDNF expression was observed in neurons in the pallidum (Figure 3), subthalamic nucleus, substantia nigra reticulata, and substantia nigra compacta (Figure 4) but not in the cortex, consistent with recent data from this laboratory[3] demonstrating transgene expression at sites known to receive anterograde projections from the putamen, but not in sites that project to the putamen. Expected widespread anterograde cortical expression of GDNF was observed in all animals treated with AAV2-GDNF in the thalamus, also consistent with our previous reports[18,19] (data not shown).

Modeling human infusion parameters

The NHP putamen cannot accommodate infusion volumes beyond ~50 µl, necessitating the use of the NHP thalamus to model infusions of the larger volumes required for coverage of the human putamen. Volumes up to 300 µl were convected successfully in the thalamus without cannula reflux or significant extrathalamic distribution of infusate. The infusion rate was increased by 1 µl/min for every 5 minutes starting at 1 µl/min to reach a maximal rate of 5 µl/min, again with no apparent change in the distribution characteristics of Gd (Figure 5a). The Vd/Vi ratio for Gd in the thalamus was 3.2 (95% CI = 0.3).

Three-dimensional reconstructions of infusions from the NHP thalamus and corresponding cannula trajectories

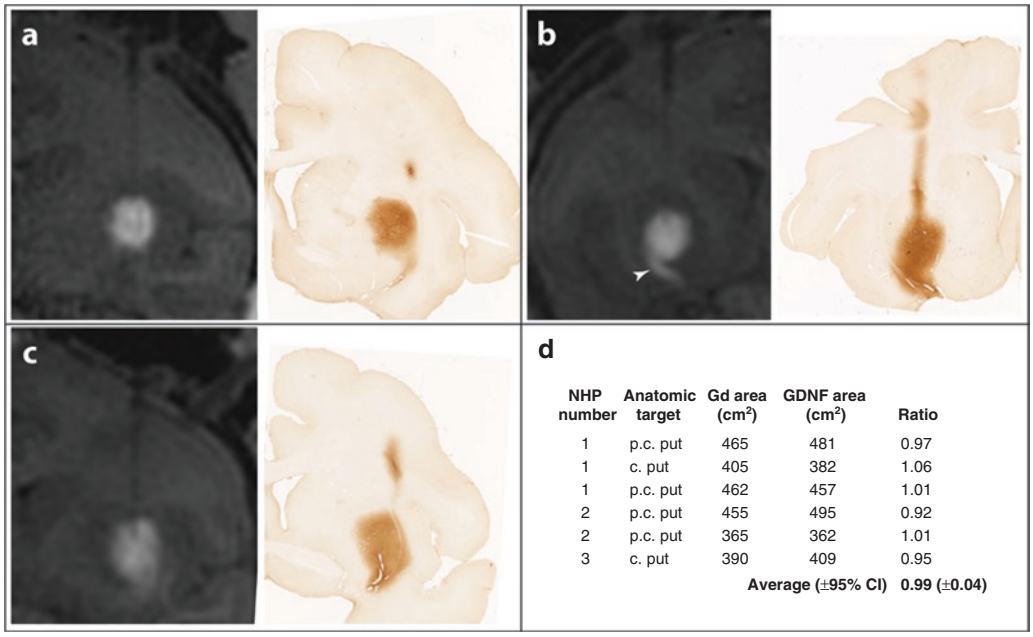

NHP number	Anatomic target	Gd area (cm^2)	GDNF area (cm^2)	Ratio
1	p.c. put	465	481	0.97
1	c. put	405	382	1.06
1	p.c. put	462	457	1.01
2	p.c. put	455	495	0.92
2	p.c. put	365	362	1.01
3	c. put	390	409	0.95
			Average (±95% CI)	0.99 (±0.04)

Figure 2 Correlation between gadoteridol (Gd) signal and glial-derived neurotrophic factor (GDNF) expression. (**a**–**c**) The center magnetic resonance imaging (MRI) slice through three separate putamenal infusions and the matching GDNF (brown) histology sections. The arrowhead in **b** denotes infusate distribution along a presumed lenticulostriate artery. The cross-sectional area values from six-matched MRI and histological slices are shown in **d**. c. put, commissural putamen; p.c., postcommissural putamen.

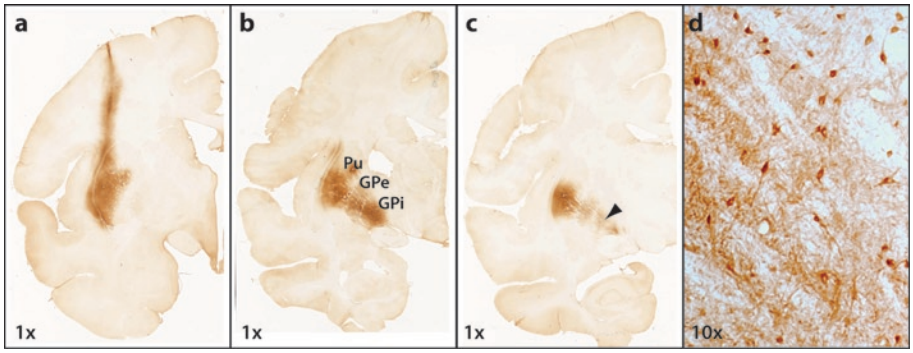

Figure 3 Anterograde transport of glial-derived neurotrophic factor (GDNF) from putamen to globus pallidus. GDNF (brown) distribution at the center of the infusion (**a**) is confined to the putamen (Pu). Anterograde transport into external globus pallidus (GPe) and internal globus pallidus (GPi) is evident at distances of (**b**) 200-µm and (**c**) 240-µm posterior to the infusion. Second order neurons are seen to express GDNF in GPi (**d**, ×10 magnification of the area indicated by the arrowhead in **c**).

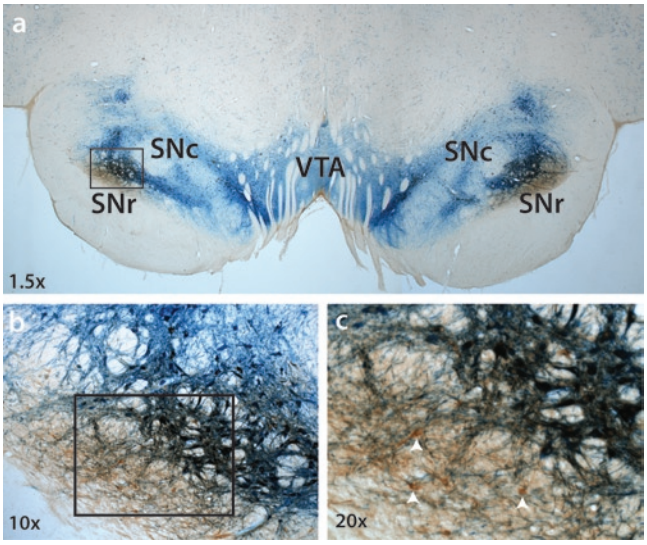

Figure 4 Anterograde transport of glial-derived neurotrophic factor (GDNF) from putamen to substantia nigra. A representative histological section at the level of the midbrain is shown in an nonhuman primates (NHP) that received bilateral putamenal adeno-associated virus serotype 2 (AAV2)-GDNF. GDNF expression (brown) primarily occurs in the area of substantia nigra reticulata (SNr), with minimal overlap into substantia nigra compacta (SNc) identified by tyrosine hydroxylase expression (blue). The box in **a** is shown at greater magnification in **b**, and the box in **b** is shown at greater magnification in **c**. Arrowheads in **c** identify neurons in SNr that express GDNF. VTA, ventral tegmental area.

(Figure 5b) were merged onto a human T2 MRI using BrainLab software. A transfrontal trajectory similar to that used previously for targeting the human putamen[20] was used to place two adjacent infusion volumes in the "green zone"[17] of the postcommissural putamen. Combinations of 150, 200, and 300 µl infusion pairs were centered along the dorsoventral putamenal axis in a manner that placed the lateral extent of the infusions at the lateral putamenal border. The maximum volume infused in the NHP thalamus, 300 µl, was contained within the anterior postcommissural putamen and pallidum, while 150 µl was the volume best contained in the posterior postcommissural location (Figure 6). Together, these two volumes covered ~60% of the total postcommissural volume.

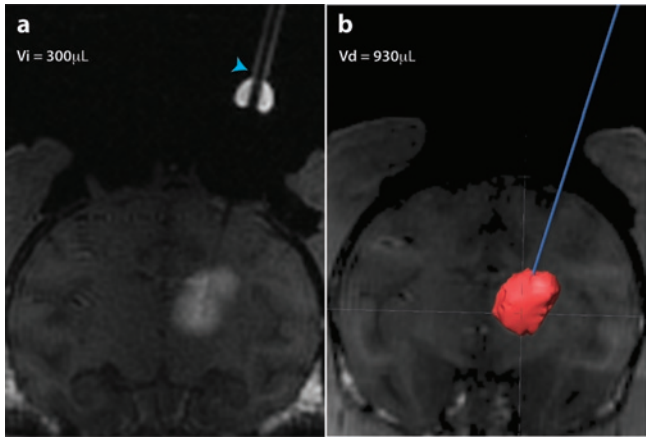

Figure 5 Rapid infusions of clinical volumes in the nonhuman primates (NHP) thalamus. (**a**) Real-time coronal magnetic resonance (MR) image obtained at the conclusion of a 300-µl volume infused at a rate of 5 µl/min. The MRI-visible trajectory guide is indicated by the arrowhead. (**b**) Three-dimensional reconstruction of the same infusion with cannula trajectory shown in blue.

DISCUSSION

In this study, we demonstrated the use of an updated clinical cannula combined with a novel, US Food and Drug Administration-approved, interventional MRI-based, skull-mounted aiming system to deliver AAV2-GDNF to the NHP putamen and thalamus in a manner analogous to that planned for a phase 1 clinical trial of putamenal AAV2-GDNF to treat PD. Within this paradigm, we confirmed previous findings that real-time imaging of coinfused Gd/AAV2-GDNF predicts the anatomic distribution of subsequent GDNF expression within the target structure. These results allow us to predict the location of cannula placement and clinical volumes most likely to achieve GDNF transgene expression in areas of the brain targeted for the treatment of PD. As a whole, this report also further indicates that human clinical trials of the direct delivery of biologics in the brain should require cannula placement using real-time MRI guidance. The rationale for a planned clinical trial, therefore, is outlined below.

Rationale for AAV2-GDNF to treat PD

CED of AAV2-GDNF was recently shown to produce clinically relevant and long-lasting regeneration of the dopaminergic

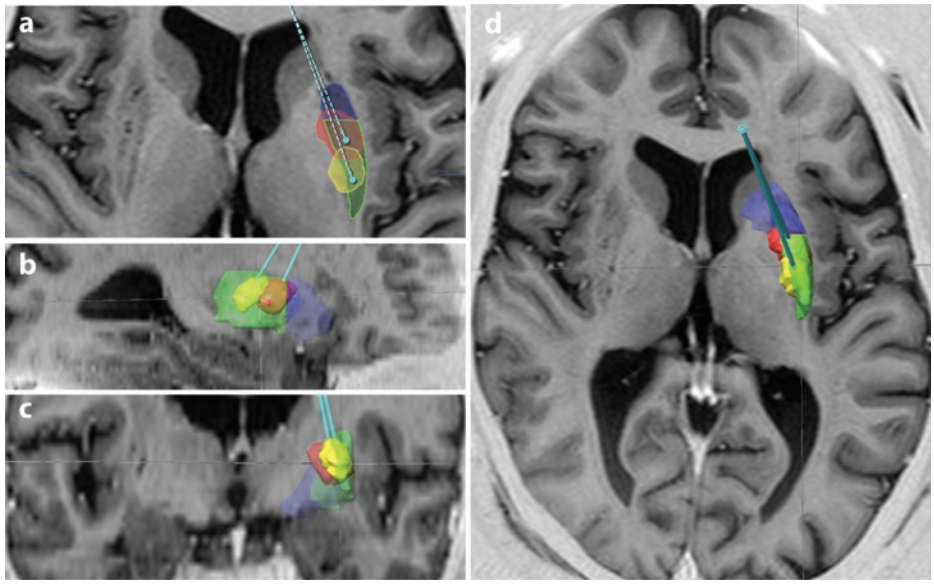

Figure 6 Three-dimensional reconstructions of nonhuman primates (NHP) thalamic infusions merged into magnetic resonance imaging (MRI)-space of human putamen. (**a**) The outlines of a 300 µl infusion (red) and a 150 µl infusion (yellow) from NHP thalamus are shown superimposed onto the human putamen, in one representative axial plan of an MRI from a Parkinson's disease (PD) patient. The precommissural putamen is shown in blue, and the postcommissural putamen is shown in green. Volumetric reconstructions of these infusions and the putamen are shown in the (**b**) lateral to medial, (**c**) posterior to anterior, and (**d**) dorsal to ventral planes.

system in rhesus macaques with stable 1-methy-4-phenyl-1,2,3,6-tetrahydropyridine (MPTP) lesions.[3] Progressive amelioration of functional deficits, recovery of dopamine levels, and regrowth of fibers to the striatal neuropil was observed in the presence of high GDNF expression, further strengthening results from previous studies in our laboratory showing that AAV2-GDNF delivered by CED is safe and effective in a NHP model of advanced PD.[4,13,21] In addition the study by Kells *et al.*[3] was unique among the preclinical literature in that initiation of neurotrophic factor gene delivery was delayed at least 3 months following MPTP administration, a timeframe during which MPTP lesioning of the nigrostriatal pathway becomes complete, to ensure a direct assessment of neuronal repair comparable to future assessments of the neurorestorative potential of GDNF in patients with PD. This body of work clearly suggests that clinical investigation of AAV2-GDNF in PD patients is warranted and, in combination with the current report, describes how this should be clinically implemented.

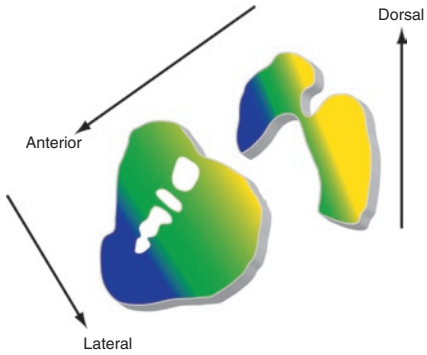

Figure 7 Diagram demonstrating the functional organization of striatal afferent projections. Colors denote functional distinctions in the organization of cortical and subcortical inputs to the striatum. Yellow, motor actions; green, premotor planning; blue, cognitive and associative functions (after Haber[45]). Yellow regions also are most susceptible to dopaminergic degeneration in Parkinson's disease.

Rationale for real-time CED of AAV2-GDNF

CED is a term that denotes the use of a continuous infusion to generate bulk flow within the brain parenchyma, *i.e.*, convection of macromolecules within the interstitial fluid driven by infusing a solution through a cannula placed directly in the targeted structure. This method allows therapeutic agents to be homogenously distributed through large volumes of brain tissue. Following the successful use of CED in preclinical studies of AAV2-aromatic L-amino acid decarboxylase in Parkinsonian NHP,[22–25] CED has been used to deliver this gene therapy to PD patients with encouraging results in two phase 1 trials.[20,26,27] In contrast, negative results were reported following the phase 2 non-CED infusion of AAV2-neurturin in Parkinson's patients.[28] Autopsy results from two patients in this non-CED trial suggested that transgene expression was achieved in only 15% of the targeted putamen. We believe the failure of neurturin to benefit patients was largely due to inadequate vector delivery, given the extensive preclinical evidence that widespread GDNF (an analog of neurturin) expression in the putamen produces significant behavioral improvement in Parkinsonian NHP when AAV2-GDNF is delivered via CED.[4,13,21]

The use of CED alone however is not adequate for ensuring optimal translation of preclinical to clinical results. An extensive analysis of the different infusion techniques used in the chronic GDNF protein infusion trials underscored the importance of variable cannula placement in producing discrepant outcomes.[11] Likewise, results from clinical trials employing CED to delivery immunotoxins[29] and chemotherapeutics[30] in brain tumor patients have also demonstrated that poor drug distribution may lead to

trial failure independent of the efficacy of the therapeutic agent.[31] For example, analysis of a subset of patients in the phase 3 clinical trial for IL13-PE38QQR, which relied on traditional image guidance for cannula placement, showed that 50% of cannulas were inaccurately placed, producing either no intracerebral infusion (30%) or poor intracerebral infusion (20%).[29] Additionally, our own analysis of infusions from AAV2-AAV2-aromatic L-amino acid decarboxylase delivered in patients by CED, without real-time visualization, suggests poor coverage of the putamen in some cases.[32]

To increase the success of translating positive results from preclinical intracerebral drug delivery studies into successful clinical trials, a method for real-time CED has evolved over several years and has been modeled extensively in NHP. Visualizing infusions in real-time provides the neurosurgeon with rapid feedback on the physical and anatomic diffusion parameters important for optimizing gene transfer and reduces the potential for adverse effects. Initially described by Oldfield and colleagues using albumin-linked surrogate tracers,[33] our current technique of real-time CED employs interventional MRI to monitor the distribution of therapeutic agents that are coinfused with gadolinium-related tracers.[34] Initial work with gadolinium-loaded liposomes[35,36] has progressed to the coinfusion of free Gd for predicting the distribution of protein[37] and AAV2 vectors.[34,36] A similar strategy, coinfusion of therapeutic agents and gadolinium-diethylenetriamene pentaacetic acid (Gd-DTPA), is used by Lonser and colleagues to treat patients with intrinsic brainstem lesions in clinical trials at the National Institutes of Health.[38]

The safety and success of real-time CED in initial clinical use, combined with preclinical data demonstrating improved control of infusate delivery and prediction of therapeutic distribution, indicate that future clinical trials of direct intracerebral drug delivery should employ this treatment strategy. In order to further maximize the potential of this technology, the present study used the ClearPoint system (SurgiVision, Irvine, CA) to deliver a custom-designed, clinical CED cannula to the target. We recently reported the initial validation of the targeting accuracy and cannula performance for this device in NHP,[14] but in the present study we have further validated the ability of the device to accurately deliver Gd/AAV2-GDNF using the exact device and protocol that will be used in an upcoming clinical trial.

Rationale for AAV2-GDNF infusion location and volume dosage

Restoration of dopaminergic function in the postcommissural region of the putamen has been the primary objective of cell transplantation and gene therapy strategies for treating patients with PD. The postcommissural and lateral precommissural putamen comprise the primary sensorimotor striatal territory (**Figure 7**), and nigrostriatal projections to this area are more sensitive to degeneration in PD than projections to associative (caudate) and limbic (nucleus accumbens) striata.[39] Although neurotrophic factor distribution within both the putamen and substantia nigra may be necessary for optimizing therapeutic potential, recent findings by our laboratory suggest that this goal can be accomplished safely and reliably by improving AAV2-GDNF infusion to the putamen alone. Two years after AAV2-GDNF delivery to the putamen, NHP showed persistent high-level expression of GDNF in the striatum and substantia nigra after broad delivery to the striatum, concurrent with stable recovery of motor function and significant functional and anatomical restoration of the dopaminergic system.[3] Furthermore, that work demonstrated that transport to the midbrain was not dependent on the integrity of the dopaminergic nigrostriatal axonal projections, confirming earlier data[18,21] demonstrating anterograde transport as the predominant mechanism for AAV2 vector translocation within the NHP brain. Because confinement of vector delivery within the putamen has been difficult to achieve previously, and cannot be verified in studies without real-time imaging, the current results are novel in showing that precisely targeted delivery of AAV2-GDNF limited to the putamen can be expected to result in robust GDNF expression in the globus pallidus and substantia nigra via anterograde transport along the striatofugal and striatonigral pathways.

We therefore planned to deliver AAV2-GDNF to two locations predicted to produce uniform distribution within the commissural/postcommissural putamen to primarily cover the sensorimotor territory. The shape of the human putamen is a challenging target for therapeutic infusions, due to its medial to lateral vertical axis and significant rostral to caudal tapering of width, which makes uniform coverage of the structure difficult without leakage into adjacent structures. We have previously shown that when the cannula step and tip are both located within a stereotactic "green zone" in the NHP that is an ~1 cm^3 volume located at least 3 mm ventral to the corpus callosum and at least 3 mm from both the internal and external capsules, 95% of the infusion can be expected to be contained within the putamen and globus pallidus.[17] In this study, suboptimal image resolution precluded definitive placement of the cannula within the green zone in some infusions where leakage occurred, although dissemination of infusate along a lenticulostriate artery was also evident in two infusions, as has previously been shown.[16] Perivascular transport and issues of cannula placement will likely be avoided with higher resolution scans available in clinical use that better delineate the vasculature and structural anatomy. Despite these issues, we demonstrated that dual infusions of 50 µl of Gd/AAV2-GDNF to the NHP putamen using this novel delivery system allows monitoring of infusate distribution and an accurate prediction of GDNF expression within the putamen that corresponds to the contained Gd distribution.

In contrast, a current strategy under clinical investigation seeks to deliver AAV2-neurturin directly to the substantia nigra in addition to putamenal delivery. In a phase 2 trial that did not meet its primary end point, patients received a total of four needle tracks per putamen to a total volume of 40 µl per hemisphere.[28] The study authors concluded that sufficient protein was not delivered to the substantia nigra, based on available postmortem histology from one patient. We believe lack of clinical efficacy was most likely due to inadequate delivery of viral vector as a result of inadequate infusion volume and use of non-CED delivery. In the subsequent AAV2-neurturin trial, however, the substantia nigra will be directly targeted. Previous reports and the current data indicate that transgene expression in the anterograde targets of substantia nigra compacta and reticulata should be anticipated as a result of AAV2 mediated delivery to the substantia nigra. If the

ventral tegmental area is primarily transduced, due to its adjacent location in the midbrain, transgene expression in its anterograde projections should be expected also. The effects of such anterograde expression of a neurotrophic transgene following delivery to the midbrain have not been carefully studies in primates. The data shown here demonstrate that maximizing the volume of delivery to the putamen using MRI-guided real-time CED should result in significant nigral transgene expression via anterograde projections from the putamen, without requiring direct midbrain delivery.

In order to scale up for predicting the optimal infusion volumes for covering the motor territory of the human putamen without extrastriatal leakage, we infused the NHP thalamus up to a maximum volume estimated to be containable within the human putamen. The human putamen has a five to six times larger volume than the rhesus putamen, indicating that 300 µl would be the upper limit for containment based on a maximum value of 50 µl in the NHP putamen. Various combinations of separate infusions of 150, 200, and 300 µl in the NHP thalamus were mapped onto the postcommissural putamen of a representative MRI from a Parkinsonian patient, so that the lateral extent of each infusion was placed at the lateral putamenal border. Risk of leakage into the external capsule dictates cannula placement closer to the medial border that will result in GDNF expression in the globus pallidus. This may be of clinical benefit, however, as delivery of the GDNF analog neurturin has previously been shown to produce behavioral improvement in Parkinsonian NHP by increasing dopamine levels in the globus pallidus.[40] GDNF also may help to restore the dopaminergic nigropallidal dopamine pathway to internal globus pallidus, proposed to represent a compensatory neuronal plasticity in early PD that is lost as the disease progresses.[41]

The resulting best-fit model utilized a 300 µl infusion within the anterior postcommissural putamen and globus pallidus, but it was necessary to use the smallest infusion volume of 150 µl in the tail of the putamen to avoid coverage of white matter tracts. **Figure 7** depicts a 300 µl infusion delivered from a cannula tip placed at anterior commissure (AC)-posterior commissure (PC) coordinates $x = 28$ mm, $y = +8$ mm, and $z = +4$ mm, and a 150 µl infusion delivered from a cannula tip placed at AC-PC coordinates $x = 30$ mm, $y = -2$ mm and $z = +5$ mm. These locations, spaced ~1 cm apart, are both within a green zone volume previously predicted for the human putamen,[17] based on minimum distances from the internal capsule, external capsule, and corpus callosum. The anterior and posterior infusions in the above model are centered ~10 and 8 mm from the internal capsule, 6 and 4 mm from the external capsule and 23 and 20 mm from the corpus callosum, respectively. Note that, ideally, the total infused volume per target site would be customized to individual patient anatomy and resultant real-time imaging data, unlike a fixed dosing regimen traditionally used in clinical trials. This modification would allow the full potential of this platform to be realized, to maximize drug delivery with optimum safety.

Note also that the infusion rate was increased in this system to a rate higher than previously possible without reflux, 5 µl/min, representing a significant reduction in procedure time for clinical protocols. Since this system allows for simultaneous bilateral infusions, the infusion times required for performing the described protocol is 45 minutes of infusion time for the anterior target and 15 minutes infusion time for the posterior target. Although higher infusion rates may be possible, a dedicated preclinical safety evaluation in NHP would be required to assess infusate delivery and tissue effects.

Efforts are underway in our lab (K.S.B.) to develop more sophisticated, MRI-based modeling software for automatically evaluating and optimizing cannula placement in individual patients, based on cannula location and anatomy-and-trajectory-specific prediction of distribution volumes. The above trajectories utilize a traditional entry point (~60–70° in the sagittal plane). A different, more anterior-to-posterior transfrontal trajectory has been used previously to place fetal dopaminergic cell grafts along the long axis of the putamen in an attempt to maximize coverage of the nucleus.[42] This approach for CED in the putamen is difficult to model in NHP. Sophisticated human modeling may determine if such an approach would be expected to significantly improve viral vector delivery, given the potential complications of anterior bifrontal trajectories.

In conclusion, this study provides guidance for optimizing parameters required to achieve widespread GDNF expression in regions of the human Parkinsonian brain. It is anticipated that this approach will be necessary for recovery of motor function in patients, using a novel, US Food and Drug Administration-approved delivery device for gene therapy. The modeling data indicate that AAV2-GDNF delivered in adjacent infusion volumes of 300 and 150 µl to the anterior and posterior postcommissural putamen, respectively, are predicted to result in GDNF expression throughout the motor area of the putamen and importantly, in the afferent regions of globus pallidus and substantia nigra. Intracerebral gene therapy clinical trials for future indications also will require real-time MRI-guided cannula placement and careful preclinical modeling of the intended protocol.

MATERIALS AND METHODS

Animals. Six adult rhesus monkeys (*Macaca mulatta*) were included in the study. Experiments were performed according to National Institutes of Health guidelines and to protocols approved by the Institutional Animal Care and Use Committee at University of California San Francisco (San Francisco, CA). NHPs were scanned on a Siemen's Magnetom Avanto 1.5T MRI (Siemens, Malvern, PA) using an array of two custom-built receive-only coils positioned on the left and right sides of the head. Using an integrated skull-mounted aiming device (SmartFrame; SurgiVision), interactive software system (ClearPoint; SurgiVision) and custom-designed clinical grade cannulas, three NHP received bilateral coinfusions of Gd (Prohance; Bracco, Milan, Italy, 1 mmol/l)/AAV2-GDNF (titer 2.3×10^{12} vector genomes/ml) into two sites in each putamen (50–60 µl per site), and three NHP received larger infusion volumes (200–300 µl) in the thalamus.

Infusion formulation. AAV2 vector containing complementary DNA sequences for human GDNF under the control of the cytomegalovirus promoter were packaged by the AAV Clinical Vector Core at Children's Hospital of Philadelphia as previously described.[43] Vector stock was diluted immediately before use to equivalent titers of 2.3×10^{12} vector genomes/ml in phosphate-buffered saline with 0.001% (vol/vol) Pluronic F-68.

Surgical procedures. Institutional regulations regarding animal studies prevented the surgical placement and removal of the skull-mounted aiming device (SmartFrame) in the iMRI suite, as would occur in patients. For this reason, 2 weeks before infusion, NHPs underwent stereotactic placement

of skull-mounted, MRI-compatible, threaded plastic adapter plugs (12 mm diameter × 14 mm height) for later attachment of the SmartFrame. After performing bilateral craniectomies, one plug was secured to the skull over each hemisphere with dental acrylic. After placement of the adapter plugs, animals recovered for at least 2 weeks before initiation of iMRI infusion procedures.

ClearPoint system. The ClearPoint system (SurgiVision) consists of the SmartFrame, an infusion cannula, and a software system that communicates with both the MRI console and the operating neurosurgeon in the MRI suite (**Figure 1**). The ClearPoint software allows registration of the AC and PC from an initial MRI scan, selection of a target for cannula tip placement in AC-PC space, and planning of the cannula trajectory (**Figure 1c–e**). Although the entry point was relatively fixed in the NHP due to use of the adapter plug, in the clinical system the entry point is modifiable in the precraniotomy planning stage as the trajectory is adjusted. The SmartFrame houses an MRI-visible (gadolinium-impregnated) fluid stem and integrated fiducials, which are detected by the software (**Figure 1c**). The fluid stem, which also serves as the infusion cannula guide, is aligned to the target trajectory via both "pitch and roll" axes and an X–Y translational stage. This is accomplished using an attached hand controller resting at the opening of the MRI bore, according to directions generated by the software in response to serial T1 MRI sequences, until the fluid stem alignment matches the chosen target trajectory.

Target selection, trajectory planning, and cannula insertion. On the day of infusion, NHP were sedated with ketamine (Ketaset, 7 mg/kg, intramuscular) and xylazine (Rompun, 3 mg/kg, intramuscular), intubated and placed on inhaled isoflurane (1–3%). The plug adapter was prepared using sterile techniques and the NHP was placed in an MRI-compatible stereotactic frame in the supine position. Vital signs were monitored throughout the procedure, and an MRI-compatible anesthesia machine was used. The SmartFrame was attached by screwing the base onto the adapter plug over one hemisphere. The NHP was moved into the bore and a controller was attached to the SmartFrame by inserting guide-wires into each of four adjustment knobs. This controller allows the surgeon to manually "dial-in" distance changes to align the cannula to the desired trajectory in four planes (pitch, roll, anterior-posterior, medial-lateral) as instructed by the ClearPoint software.

First, a high-resolution anatomical MR scan was acquired for target identification and surgical planning. The scan was a 9-minute three-dimensional magnetization prepared rapid gradient echo acquired with near-isotropic voxel dimensions of 0.7 × 0.7 × 1 mm over a 180 mm field of view with 128 slices, an echo time of 3.76 ms, an inversion time of 1,100 ms, a repetition time of 2,170 ms, a 15° flip angle and a bandwidth of 130 Hz/pixel. The three-dimensional magnetization prepared rapid gradient echo images were then transferred to the ClearPoint system, where the target for cannula tip placement was selected. In three animals, one intraputamenal location at the level of the AC and one postcommissural location were selected bilaterally.

Next, rapid scans were obtained that allowed the ClearPoint software to detect the position and orientation of the SmartFrame fluid stem. First, a 6-second two-dimensional turbo-spin echo was acquired through the distal fluid stem in an orientation perpendicular to the desired trajectory. The scan was acquired at 1 mm in-plane resolution over a 128 mm field of view with a single 10-mm thick, a echo time of 41 ms, repetition time of 704 ms, 2 repetitions, an echo train length of 37 and a bandwidth of 400 Hz/pixel. The software used in this image to compare the current SmartFrame trajectory to the target trajectory in order to calculate an expected error for tip placement and generate instructions to adjust SmartFrame alignment via the pitch and roll. After these adjustments were made, the scan was reacquired to measure the new expected error and this process was repeated if necessary.

When the expected error fell <1.0 mm, the pitch and roll axes on the SmartFrame were locked and a 26 second two-dimensional turbo-spin echo scan was acquired along the sagittal and coronal planes of the guide stem for fine adjustment of the SmartFrame X–Y stage. Seven slices of 1-mm isotropic resolution were acquired over a 180 × 240 mm field of view with a echo time of 22 ms, a repetition time of 500 ms, 2 repetitions, an echo train length of 7 and a bandwidth 250 of Hz/pixel. The ClearPoint software used in these images to generate instructions for fine adjustment of the trajectory, achieved by dialing-in distance changes on the SmartFrame X–Y stage. This process was repeated until the software reported an expected error of <0.5 mm, which typically required no more than two iterations.

The infusion system included a custom-designed, ceramic, fused silica reflux-resistant cannula with a 3 mm stepped tip that was developed in accordance with previously reported principles developed in our laboratory.[35,44] Cannula was attached to a 1-ml syringe mounted onto a MRI-compatible infusion pump (Harvard Bioscience, Hollistan, MA). With the aiming device aligned in its final position, the software reported the distance from the target to the top of the guide stem, and this distance was measured from the cannula tip and marked on the cannula using a sterile ink marker. A depth stop was then secured at the marked location and the measured insertion distance was verified. The infusion pump was started at 1 µl/min, and after visualizing fluid flow from the cannula tip when held at the height of the bore, the cannula was inserted through the SmartFrame guide stem and into the brain. When the depth stop encountered the top of the guide stem, it was secured with a locking screw.

Infusion and imaging. Following cannula insertion, repeated multiplanar fast low angle shot images were obtained every 5 minutes throughout the duration of the infusion. The fast low angle shot images were acquired at an in-plane resolution of 0.7 × 0.7 × 1 mm with 128 slices over the 180 mm field of view at a echo time of 4.49 ms, a repetition time of 17 ms with 2 repetitions, and a bandwidth of 160 Hz/pixel. The first scan was acquired with a 4° flip angle to produce a proton-density weighted image for visualization of the cannula tip. All subsequent scans were acquired with a 40° flip angle to increase the T1-weighting and highlight the signal enhancement from Gd in the infusate.

Upon visualization of Gd infusion at the cannula tip, the infusion rates were increased from an initial rate of 1 µl/min in a ramping fashion, 0.5 µl/min every 5 minutes, to reach a maximum of 3 µl/min (putamen infusions) or increased from an initial rate of 1 µl/min in a ramping fashion, 1 µl/min every 5 minutes, to reach a maximum of 5 µl/min (thalamus infusions). The infusion rate was determined prospectively, based on prior experience.[14]

Imaging data analysis. Images obtained during RCD were transferred to the ClearPoint system for analysis of targeting error. With the target position hidden from view, the location of the cannula tip was manually selected in the ClearPoint console by identifying the center of the Gd signal in the lower one-third of the infusion volume on the first scan demonstrating convection following cannula insertion (**Figure 4f**). The software then automatically reported the vector distance between the target site and the actual position of the cannula tip. The average target error for all infusions was later calculated and the 95% CI was determined.

Distribution volumes of Gd were measured using Osirix, an open-source DICOM reader and imaging workstation. Software was written and applied as an Osirix plug-in to autosegment each infusion on individual, baseline-subtracted MRI slices from which a total infusion volume was automatically calculated.

Images obtained during RCD also were transferred to an iPlan workstation (BrainLab, Feldkirchen, Germany) to generate three-dimensional reconstructions of infusion volumes. Reconstructed volumes from one animal infused in the thalamus were merged to an MRI from an anonymous patient with PD.

Tissue processing. Each NHP was perfused transcardially 5 weeks after AAV2-GDNF infusion with cold saline followed by 4% paraformaldehyde. Brains were harvested, sliced in 6 mm coronal sections in a brain matrix, postfixed overnight in 4% paraformaldehyde and cryoprotected in 30% sucrose. A sliding microtome was used to cut 40-µm serial sections for histological processing. For GDNF immunohistochemistry, sections were first washed three times in phosphate-buffered solution for 5 minutes each followed by treatment with 1% H_2O_2 in phosphate-buffered solution for 20 minutes at room temperature. Sections were then incubated in Sniper blocking solution (Biocare Medical, Concord, CA) for 30 minutes at room temperature followed by incubation with primary antibody (goat polyclonal anti-GDNF, 1:500; R&D Systems) in Da Vinci diluent (Biocare Medical) overnight at room temperature. After three washes in phosphate-buffered solution with 0.01% Tween-20, sections were sequentially incubated in Goat Probe and Goat Polymer HRP (Biocare Medical) for 1 hour each at room temperature, followed by several washes and colorimetric development with 3,30-diaminobenzidine. Immunostained sections were mounted on slides and sealed with Cytoseal (Richard-Allan Scientific, Kalamazoo, MI). Double labeling immunohistochemistry for GDNF and tyrosine hydroxylase was performed as for GDNF alone with the addition of mouse monoclonal anti-tyrosine hydroxylase (1:5,000; Chemicon, Billerica, MA) to the primary antibody incubation, Mach 2 Mouse AP (Biocare Medical) to the goat polymer and staining with Vector Blue AP after 3,30-diaminobenzidine development.

Analysis of GDNF expression. The analysis of GDNF expression was performed by light microscopy as previously described (Su 2010). GDNF-positive areas were identified at low magnification and positively stained cells were confirmed under high magnification. Areas staining positive for GDNF were transferred to the corresponding primate MRI by manually delineating positive areas on the corresponding baseline MRI images using OsiriX software, without reference to the MR images showing Gd distribution. Regions of interest were delineated separately for GDNF expression and Gd distribution by two independent senior observers.

ACKNOWLEDGMENT

This work was supported in part by an NIH award F32 NS064692 (R.M.R.), and the Michael J. Fox Foundation (K.S.B.).

REFERENCES

1. Love, S, Plaha, P, Patel, NK, Hotton, GR, Brooks, DJ and Gill, SS (2005). Glial cell line-derived neurotrophic factor induces neuronal sprouting in human brain. *Nat Med* **11**: 703–704.
2. Ai, Y, Markesbery, W, Zhang, Z, Grondin, R, Elseberry, D, Gerhardt, GA *et al.* (2003). Intraputamenal infusion of GDNF in aged rhesus monkeys: distribution and dopaminergic effects. *J Comp Neurol* **461**: 250–261.
3. Kells, AP, Eberling, J, Su, X, Pivirotto, P, Bringas, J, Hadaczek, P *et al.* (2010). Regeneration of the MPTP-lesioned dopaminergic system after convection-enhanced delivery of AAV2-GDNF. *J Neurosci* **30**: 9567–9577.
4. Eberling, JL, Kells, AP, Pivirotto, P, Beyer, J, Bringas, J, Federoff, HJ *et al.* (2009). Functional effects of AAV2-GDNF on the dopaminergic nigrostriatal pathway in parkinsonian rhesus monkeys. *Hum Gene Ther* **20**: 511–518.
5. Nutt, JG, Burchiel, KJ, Comella, CL, Jankovic, J, Lang, AE, Laws, ER Jr *et al.* (2003). Randomized, double-blind trial of glial cell line-derived neurotrophic factor (GDNF) in PD. *Neurology* **60**: 69–73.
6. Gill, SS, Patel, NK, Hotton, GR, O'Sullivan, K, McCarter, R, Bunnage, M *et al.* (2003). Direct brain infusion of glial cell line-derived neurotrophic factor in Parkinson disease. *Nat Med* **9**: 589–595.
7. Patel, NK, Bunnage, M, Plaha, P, Svendsen, CN, Heywood, P and Gill, SS (2005). Intraputamenal infusion of glial cell line-derived neurotrophic factor in PD: a two-year outcome study. *Ann Neurol* **57**: 298–302.
8. Lang, AE, Gill, S, Patel, NK, Lozano, A, Nutt, JG, Penn, R *et al.* (2006). Randomized controlled trial of intraputamenal glial cell line-derived neurotrophic factor infusion in Parkinson disease. *Ann Neurol* **59**: 459–466.
9. Marks, WJ Jr, Ostrem, JL, Verhagen, L, Starr, PA, Larson, PS, Bakay, RA *et al.* (2008). Safety and tolerability of intraputaminal delivery of CERE-120 (adeno-associated virus serotype 2-neurturin) to patients with idiopathic Parkinson's disease: an open-label, phase I trial. *Lancet Neurol* **7**: 400–408.
10. Salvatore, MF, Ai, Y, Fischer, B, Zhang, AM, Grondin, RC, Zhang, Z *et al.* (2006). Point source concentration of GDNF may explain failure of phase II clinical trial. *Exp Neurol* **202**: 497–505.
11. Morrison, PF, Lonser, RR and Oldfield, EH (2007). Convective delivery of glial cell line-derived neurotrophic factor in the human putamen. *J Neurosurg* **107**: 74–83.
12. Tatarewicz, SM, Wei, X, Gupta, S, Masterman, D, Swanson, SJ and Moxness, MS (2007). Development of a maturing T-cell-mediated immune response in patients with idiopathic Parkinson's disease receiving r-metHuGDNF via continuous intraputaminal infusion. *J Clin Immunol* **27**: 620–627.
13. Su, X, Kells, AP, Huang, EJ, Lee, HS, Hadaczek, P, Beyer, J *et al.* (2009). Safety evaluation of AAV2-GDNF gene transfer into the dopaminergic nigrostriatal pathway in aged and parkinsonian rhesus monkeys. *Hum Gene Ther* **20**: 1627–1640.
14. Richardson, RM, Kells, AP, Martin, AJ, Larson, PS, Starr, PA, Piferi, PG *et al.* (2011). Novel platform for MRI-guided convection-enhanced delivery of therapeutics: preclinical validation in nonhuman primate brain. Stereotact Funct Neurosurg, in press.
15. Su, X, Kells, AP, Aguilar Salegio, EA, Richardson, RM, Hadaczek, P, Beyer, J *et al.* (2010). Real-time MR imaging with Gadoteridol predicts distribution of transgenes after convection-enhanced delivery of AAV2 vectors. *Mol Ther* **18**: 1490–1495.
16. Krauze, MT, Saito, R, Noble, C, Bringas, J, Forsayeth, J, McKnight, TR *et al.* (2005). Effects of the perivascular space on convection-enhanced delivery of liposomes in primate putamen. *Exp Neurol* **196**: 104–111.
17. Yin, D, Valles, FE, Fiandaca, MS, Bringas, J, Gimenez, F, Berger, MS *et al.* (2011). Optimal region of the putamen for image-guided convection-enhanced delivery of therapeutics in human and non-human primates. *Neuroimage* **54** Suppl 1: S196–S203.
18. Kells, AP, Hadaczek, P, Yin, D, Bringas, J, Varenika, V, Forsayeth, J *et al.* (2009). Efficient gene therapy-based method for the delivery of therapeutics to primate cortex. *Proc Natl Acad Sci USA* **106**: 2407–2411.
19. Salegio, EA, Kells, AP, Richardson, RM, Hadaczek, P, Forsayeth, J, Bringas, J *et al.* (2010) MRI-guided delivery of AAV2 to the primate brain for the treatment of lysosomal storage disorders. *Hum Gene Ther* **21**: 1093–1103.
20. Eberling, JL, Jagust, WJ, Christine, CW, Starr, P, Larson, P, Bankiewicz, KS *et al.* (2008). Results from a phase I safety trial of hAADC gene therapy for Parkinson disease. *Neurology* **70**: 1980–1983.
21. Johnston, LC, Eberling, J, Pivirotto, P, Hadaczek, P, Federoff, HJ, Forsayeth, J *et al.* (2009). Clinically relevant effects of convection-enhanced delivery of AAV2-GDNF on the dopaminergic nigrostriatal pathway in aged rhesus monkeys. *Hum Gene Ther* **20**: 497–510.
22. Bankiewicz, KS, Eberling, JL, Kohutnicka, M, Jagust, W, Pivirotto, P, Bringas, J *et al.* (2000). Convection-enhanced delivery of AAV vector in parkinsonian monkeys; *in vivo* detection of gene expression and restoration of dopaminergic function using pro-drug approach. *Exp Neurol* **164**: 2–14.
23. Bankiewicz, KS, Forsayeth, J, Eberling, JL, Sanchez-Pernaute, R, Pivirotto, P, Bringas, J *et al.* (2006). Long-term clinical improvement in MPTP-lesioned primates after gene therapy with AAV-hAADC. *Mol Ther* **14**: 564–570.
24. Daadi, MM, Pivirotto, P, Bringas, J, Cunningham, J, Forsayeth, J, Eberling, J *et al.* (2006). Distribution of AAV2-hAADC-transduced cells after 3 years in Parkinsonian monkeys. *Neuroreport* **17**: 201–204.
25. Forsayeth, JR, Eberling, JL, Sanftner, LM, Zhen, Z, Pivirotto, P, Bringas, J *et al.* (2006). A dose-ranging study of AAV-hAADC therapy in Parkinsonian monkeys. *Mol Ther* **14**: 571–577.
26. Christine, CW, Starr, PA, Larson, PS, Eberling, JL, Jagust, WJ, Hawkins, RA *et al.* (2009). Safety and tolerability of putaminal AADC gene therapy for Parkinson disease. *Neurology* **73**: 1662–1669.
27. Muramatsu, S, Fujimoto, K, Kato, S, Mizukami, H, Asari, S, Ikeguchi K *et al.* (2010) A phase I study of aromatic L-amino acid decarboxylase gene therapy for Parkinson's disease. *Mol Ther* **18**: 1731–1735.
28. Lidar, Z, Mardor, Y, Jonas, T, Pfeffer, R, Faibel, M, Nass, D *et al.* (2004). Convection-enhanced delivery of paclitaxel for the treatment of recurrent malignant glioma: a phase I/II clinical study. *J Neurosurg* **100**: 472–479.
29. Sampson, JH, Archer, G, Pedain, C, Wembacher-Schröder, E, Westphal, M, Kunwar,S *et al.* (2010). Poor drug distribution as a possible explanation for the results of the PRECISE trial. *J Neurosurg* **113**: 301–309.
30. Lidar, Z, Mardor, Y, Jonas, T, Pfeffer, R, Faibel, M, Nass, D *et al.* (2004). Convection-enhanced delivery of paclitaxel for the treatment of recurrent malignant glioma: a phase I/II clinical study. *J Neurosurg* **100**: 472–479.
31. Sampson, JH, Raghavan, R, Provenzale, JM, Croteau, D, Reardon, DA, Coleman, RE *et al.* (2007). Induction of hyperintense signal on T2-weighted MR images correlates with infusion distribution from intracerebral convection-enhanced delivery of a tumor-targeted cytotoxin. *AJR Am J Roentgenol* **188**: 703–709.
32. Valles, F, Fiandaca, MS, Eberling, JL, Starr, PA, Larson, PS, Christine, CW *et al.* (2010). Qualitative imaging of adeno-associated virus serotype 2-human aromatic L-amino acid decarboxylase gene therapy in a phase I study for the treatment of Parkinson disease. *Neurosurgery* **67**: 1377–1385.
33. Nguyen, TT, Pannu, YS, Sung, C, Dedrick, RL, Walbridge, S, Brechbiel, MW *et al.* (2003). Convective distribution of macromolecules in the primate brain demonstrated using computerized tomography and magnetic resonance imaging. *J Neurosurg* **98**: 584–590.
34. Richardson, RM, Varenika, V, Forsayeth, JR and Bankiewicz, KS (2009). Future applications: gene therapy. *Neurosurg Clin N Am* **20**: 205–210.
35. Fiandaca, MS, Forsayeth, JR, Dickinson, PJ and Bankiewicz, KS (2008). Image-guided convection-enhanced delivery platform in the treatment of neurological diseases. *Neurotherapeutics* **5**: 123–127.
36. Fiandaca, MS, Varenika, V, Eberling, J, McKnight, T, Bringas, J, Pivirotto, P *et al.* (2009). Real-time MR imaging of adeno-associated viral vector delivery to the primate brain. *Neuroimage* **47 Suppl 2**: T27–T35.
37. Gimenez, F, Krauze, MT, Valles, F, Hadaczek, P, Bringas, J, Sharma, N *et al.* (2011). Image-guided convection-enhanced delivery of GDNF protein into monkey putamen. *Neuroimage* **54 Suppl 1**: S189–S195.

38. Lonser, RR, Warren, KE, Butman, JA, Quezado, Z, Robison, RA, Walbridge, S *et al.* (2007). Real-time image-guided direct convective perfusion of intrinsic brainstem lesions. Technical note. *J Neurosurg* **107**: 190–197.
39. Smith, Y and Villalba, R (2008). Striatal and extrastriatal dopamine in the basal ganglia: an overview of its anatomical organization in normal and Parkinsonian brains. *Mov Disord* **23 Suppl 3**: S534–S547.
40. Grondin, R, Zhang, Z, Ai, Y, Ding, F, Walton, AA, Surgener, SP *et al.* (2008). Intraputamenal infusion of exogenous neurturin protein restores motor and dopaminergic function in the globus pallidus of MPTP-lesioned rhesus monkeys. *Cell Transplant* **17**: 373–381.
41. Whone, AL, Moore, RY, Piccini, PP and Brooks, DJ (2003). Plasticity of the nigropallidal pathway in Parkinson's disease. *Ann Neurol* **53**: 206–213.
42. Freed, CR, Greene, PE, Breeze, RE, Tsai, WY, DuMouchel, W, Kao, R *et al.* (2001). Transplantation of embryonic dopamine neurons for severe Parkinson's disease. *N Engl J Med* **344**: 710–719.
43. Wright, JF, Qu, G, Tang, C and Sommer, JM (2003). Recombinant adeno-associated virus: formulation challenges and strategies for a gene therapy vector. *Curr Opin Drug Discov Devel* **6**: 174–178.
44. Krauze, MT, Saito, R, Noble, C, Tamas, M, Bringas, J, Park, JW *et al.* (2005). Reflux-free cannula for convection-enhanced high-speed delivery of therapeutic agents. *J Neurosurg* **103**: 923–929.
45. Haber, SN (2003). The primate basal ganglia: parallel and integrative networks. *J Chem Neuroanat* **26**: 317–330.